Classification of instabilities in the flow past flexible surfaces

V. Kumaran

Department of Chemical Engineering, Indian Institute of Science, Bangalore 560 012, India

The stability of the laminar flow in flexible tubes and channels could be influenced by the flexibility of the walls, and these instabilities are qualitatively different from those in rigid tubes and channels. In this paper, the instabilities of the laminar flow in flexible tubes and channels are classified according to the asymptotic regime in which they are observed, the flow structure, the scaling of the critical Reynolds number (rVR/m) with the dimensionless parameter $\Sigma = (rGR^2/m^2)$, and the mechanism that destabilizes the flow. Here, r and m are the fluid density and viscosity, G is the shear modulus of the wall material, R is the cross stream length scale and V is the maximum velocity. Three types of instabilities have been analysed. The viscous instability is observed in the limit of low Reynolds number when the fluid inertia is insignificant, and the critical Reynolds number scales as $Re \propto \Sigma$. The destabilizing mechanism is the transfer of energy from the mean flow to the fluctuations due to the shear work done by the mean flow at the surface. In the high Reynolds number inviscid modes, the critical Reynolds number scales are $Re \propto \Sigma^{1/2}$, and there is a critical layer of thickness $Re^{-1/3}$ where viscous stresses are important. The destabilizing mechanism is the transfer of energy from the mean flow to the fluctuations due to the Reynolds stresses in the critical layer. The high Reynolds number wall mode instability has a wall layer of thickness $Re^{-1/3}$ at the wall, where viscous stresses are important and the critical Reynolds number scales as $Re \propto \Sigma^{3/4}$. The destabilizing mechanism is the transfer of energy from the mean flow to the fluctuations due to the shear work done by the mean flow at the interface.

Introduction

The laminar–turbulent transition in flows past compliant surfaces has been extensively studied due to its importance in marine and aerospace applications. In these applications, it is desirable to reduce the drag force exerted by flow, and the transition delay due to compliant walls has been a potential candidate for drag reduction. The first studies in this area were carried out by Kramer[1,2], who speculated that the efficiency of swimming of dolphins was due to the transition delay induced by the compliant nature of their skins. Though the original mechanism suggested by Kramer is in doubt[3,4], there has been a lot of subsequent theoretical and experimental work on the transition delay in flows past compliant surfaces. The first theoretical studies on the effect of a compliant wall on flow stability were carried out by Benjamin[5,6] and Landahl[7]. By extending the stability theory of Tollmien[8] and Schlichting[9] for the flow past rigid surfaces, Benjamin[5] showed that a flexible non-dissipative wall tends to stabilize the Tollmien-Schlichting instability, which is the destabilizing mechanism in the flow past a rigid surface. In addition, Benjamin[5] and Landah[7] also pointed out that there is an additional mode of instability that could exist in an inviscid flow, which was termed the flow-induced surface instability. Since then, there has been much work on the flow past a Kramer-type surface[3,4,10,11]. Most of the subsequent studies have determined the stability by a numerical solution of the Orr-Sommerfeld equation for the fluid velocity, which requires sophisticated numerical techniques due to the stiffness of the governing equation. An asymptotic analysis was used[10] to obtain the stability characteristics when the critical layer near the wall is well separated from the viscous sublayer, and Carpenter and Garrad[4] used a potential flow calculation to derive approximate stability criteria. The consensus appears to be that a compliant wall does indeed lead to drag reduction due to a postponement in the transition from laminar to turbulent flow. A numerical study of the effect of flexible walls on the stability of a plane Poiseuille flow was carried out[12], using an extension of the techniques developed by Lin[13]. However, there does not appear to be much work on the flow through a tube bounded by a flexible wall. In part, this may be because the linear stability analysis predicts that the fully developed flow is stable, and the Tollmien-Schlichting instability does not exist for a rigid tube.

While the above studies have been motivated by marine and aerospace applications, flows in flexible tubes and channels are also encountered in biological applications. The Reynolds number in the latter case is relatively low compared to those encountered in marine and aerospace applications, and fluid inertia could even be negligible in some cases. There have been relatively

e-mail: kumaran@chemeng.iisc.ernet.in

few studies in parameter regimes of interest in biological applications. The first experimental studies appear to have been carried out by Krindel and Silberberg[14], who examined the pressure drop required for flow in a gel walled tube. They came to the surprising conclusion that the laminar flow in a gel walled tube becomes unstable at a Reynolds number lower than the value of 2100 for a rigid tube, and instability appeared to be accompanied by oscillations in the wall of the tube. Motivated by this, a series of linear stability studies in various parameter regimes were carried out[15–28] for the flow in tubes and channels bounded by gel walls. The results of these studies indicated that there are at least three modes of instability in flexible walled channels and tubes which are qualitatively different from those in rigid channels and tubes. More recently, experimental confirmation of the 'viscous instability' in the limit where fluid inertia is negligible has been reported[29,30], and a nonlinear analysis of the viscous instability has also been carried out[31]. The classification of these instabilities is the subject of the present paper, and particular attention is focused on the asymptotic regime where these are observed, the flow structure and the destabilizing mechanism. Attention is restricted to linear stability analyses of the flow past gel walled tubes and channels, since this has been the most comprehensively studied problem.

Methodology

The configurations for the base flow in a gel walled tube and channel are shown in Figure 1. The equations governing the fluid flow are the incompressible Navier-Stokes equations

$$\nabla.\mathbf{v} = 0 \tag{1}$$

$$\mathbf{r}(\partial_t \mathbf{v} + \mathbf{v}.\nabla \mathbf{v}) = -\nabla p + \mathbf{m}\nabla^2 \mathbf{v}, \tag{2}$$

where $\mathbf{v}$ and p are the velocity and pressure fields, $\mathbf{r}$ and $\mathbf{m}$ are the fluid density and viscosity respectively, and ∂_t represents the time derivative. The dynamics of the flexible wall is represented by a displacement field $\mathbf{u}$, which is the displacement of material points from their steady state positions due to fluctuations in the fluid stresses at the interface. The displacement field is governed by linear elasticity equations for an incompressible material

$$\nabla.\mathbf{u} = 0 \tag{3}$$

$$\mathbf{r}\partial_t^2 \mathbf{u} = -\nabla p + G\nabla^2 \mathbf{u} + \mathbf{m_g}\nabla^2(\partial_t \mathbf{u}). \tag{4}$$

In the above equation, the left side is the rate of change of momentum due to acceleration, and the density of the wall material is assumed to be equal to that of the fluid. The first term on the right is the gradient of a pressure which is required to ensure incompressibility. The second term on the right is the divergence of an elastic stress,

$$\mathbf{s}_e = G(\nabla\mathbf{u} + (\nabla\mathbf{u})^T), \tag{5}$$

where G is the coefficient of elasticity. The third term on the right side of eq. (4) is the divergence of a viscous stress,

$$\mathbf{s}_v = \mathbf{m_g}(\nabla\partial_t \mathbf{u} + (\nabla\partial_t \mathbf{u})^T), \tag{6}$$

where $\partial_t \mathbf{u}$ is the velocity field on the wall material, and $\mathbf{m_g}$ is the viscosity. The boundary conditions at the interface between the wall material and the rigid surface are zero displacement conditions $\mathbf{u} = 0$, while the boundary conditions between a rigid surface and the fluid are the no-slip conditions $\mathbf{v} = \mathbf{v}_s$, where $\mathbf{v}_s$ is the velocity of the surface. Continuity of velocity and continuity of stress conditions are applied at the interface between the fluid and the wall material.

In the linear stability analysis, small perturbations $\mathbf{v}'$ and $\mathbf{u}'$ are placed on the base state velocity and displacement field. The base flow for a channel is a plane Couette flow

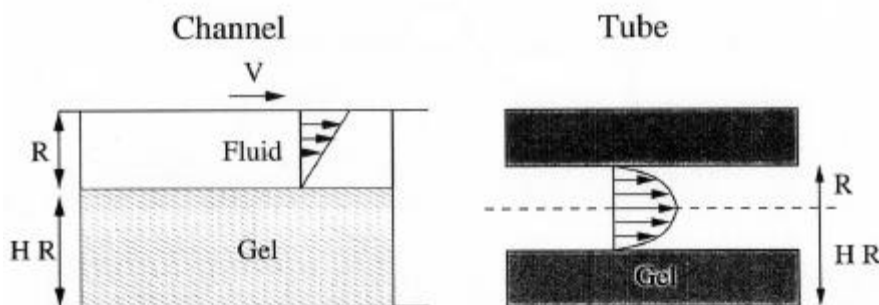$$\bar{v}_x = \frac{V_z}{R} \quad \bar{v}_z = 0, \tag{7}$$

Figure 1. Configurations and coordinate systems used for analysing the flow past flexible surfaces.

and the perturbations are the form

$$\begin{pmatrix} \mathbf{v}' \\ \mathbf{u}' \end{pmatrix} = \begin{pmatrix} \tilde{\mathbf{v}}(z) \\ \tilde{\mathbf{u}}(z) \end{pmatrix} \exp{(ikx + st)}, \tag{8}$$

where x and z are the flow and gradient directions respectively, k is the wave number in the flow direction and s is the growth rate. For a tube (Figure 1 b), the base flow is a Hagen-Poiseuille flow

$$\bar{v}_x = V\left(1 - \frac{r^2}{R^2}\right) \bar{v}_r = 0, \tag{9}$$

$$\begin{pmatrix} \mathbf{v}' \\ \mathbf{u}' \end{pmatrix} = \begin{pmatrix} \tilde{\mathbf{v}}(r) \\ \tilde{\mathbf{u}}(r) \end{pmatrix} \exp{(ikx + in\theta + st)}, \tag{10}$$

where r, $\boldsymbol{q}$ and x are the radial, azimuthal and axial coordinates in a cylindrical coordinate system with axis along the centerline of the tube. The above form of the perturbations is inserted into the conservation equations, and the solutions for the perturbations $\tilde{\mathbf{u}}$ and $\tilde{\mathbf{v}}$ which are consistent with the boundary conditions at the rigid surfaces are determined as a function of wave number k and the growth rate s. These are inserted into the velocity and stress boundary conditions at the interface between the fluid and the wall material, and the dispersion matrix is determined. The determinant of this matrix is set equal to zero in order to determine the growth rate s. The perturbations are stable if the real part of the growth rate is negative, and they are unstable if the real part is positive. The transition from stable to unstable modes takes place when the real part of the growth rate passes through zero.

There are reasons to expect that the instability of the flow past a flexible surface could be very different from that for the flow past a rigid surface.

1. In addition to the Reynolds number $Re = (\boldsymbol{r}VR/\boldsymbol{m})$, which is the ratio of inertial and viscous forces, there are three additional dimensionless parameters, the ratio of elastic and viscous forces $\Sigma = (\boldsymbol{r}GR^2/\boldsymbol{m}^2)$, the ratio of viscosities $\boldsymbol{m}_r = (\boldsymbol{m}_g/\boldsymbol{m})$, and the ratio of the thickness of the fluid and wall material. This implies that there is more than one parameter that can be modified to induce or delay instability, in contrast to flows past rigid surfaces where the Reynolds number is the only parameter which determines the stability of the flow.

2. Another important difference between the flow past rigid and flexible surfaces is that a normal velocity is permitted at a flexible surface. Many of the classical theorems of hydrodynamic stability, such as the Rayleigh and Fjortoft theorems[32], are not valid for flow past flexible surfaces because

they assume that the normal velocity is zero at the wall. Consequently, the flow past a flexible surface could go unstable in parameter regimes where the theorems of hydrodynamic instability would predict that the flow past a rigid surface is stable.

3. In the flow past a rigid surface, the coupling between the mean flow and the fluctuations is due to the nonlinear inertial term in the momentum conservation eq. (2), and the destabilizing mechanism is the transfer of energy between the mean flow and the fluctuations due to the Reynolds stresses. In the flow past a flexible surface, additional couplings arise due to the variation of the mean velocity at the fluid–wall interface caused by the displacement of the surface. This results in an additional mode of transport of energy from the mean flow to the fluctuations due to the shear work done by the mean flow at the interface, which could also destabilize the flow.

Therefore, the instability of the flow past a flexible surface is not just a modification of the rigid flow instability, but could be qualitatively different.

The linear stability equations for the fluid and the wall material are difficult to solve analytically, except in certain asymptotic limits. Therefore, it is necessary to obtain analytical results in asymptotic limits, and extend the calculation numerically in the intermediate regime. The asymptotic limits where an instability occurs, and the physical mechanism for the instability, are summarized here.

Viscous instability

The viscous instability in the flow past a flexible surface was first reported by Kumaran et al.[15] for the Couette flow past a flexible surface (Figure 1 a), and subsequently analysed[16] for the flow in a flexible tube. More recently, a nonlinear analysis was carried out by Shankar and Kumaran[27], and experimental studies[29,30] have also confirmed the existence of this instability. In the low Reynolds number limit, the inertial terms in the conservation equation are neglected, and the Stokes equations for the fluid in this limit are

$$\nabla \cdot \mathbf{v} = 0, \tag{11}$$

$$-\nabla p + \boldsymbol{m}\nabla^2 \mathbf{v} = 0, \tag{12}$$

If the Reynolds number is set equal to zero, the only dimensionless parameters which affect the dynamics of the perturbations are $\Gamma = (V\boldsymbol{m}/GR)$, which is the ratio of viscous forces in the fluid and elastic focus in the wall material, and the ratio of viscosities $\boldsymbol{m}_r$ and the ratio of the thickness of the wall and the fluid layers.
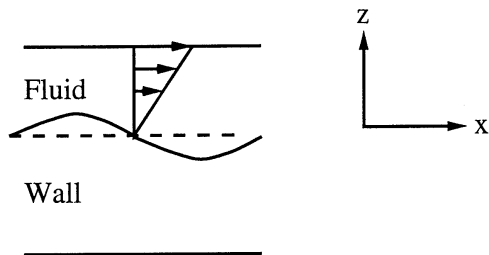
Figure 2. Mechanism of viscous instability in the flow past flexible surfaces.

There is no instability in the zero Reynolds number limit for the flow past a rigid surface, because the non-linear inertial terms in the conservation equation which couples the mean flow to the fluctuations is not present. In addition, the Stokes equations are quasi steady, and do not contain any explicit time dependence. The dynamics in the flow past a flexible surface is qualitatively different, because the time dependence enters through the elastic terms in the conservation equations for the wall material. There is also a coupling between the mean flow and the fluctuations in the tangential velocity boundary condition at the interface, due to the variation in the mean velocity with height. This can be explained as follows. Consider the interface between a fluid and a flexible surface as shown in Figure 2. The tangential velocity continuity condition for this configuration is applied at the displaced interface $z = u_z$ for a plane Couette flow

$$V_x|_{z = u_z} = (\partial_t u_x)|_{u_z}, \tag{13}$$

where V_x is the tangential velocity at the surface, and u_x is the tangential displacement field. In the linear approximation, the above equation is linearized using a Taylor series expansion about $z = 0$ to obtain, correct to first order in the perturbations to the displacement and velocity fields,

$$v'_x|_{z=0} + u'_z \frac{d\overline{v}}{dz}\bigg|_{z=0} = (\partial_t u'_x)|_{z=0}. \tag{14}$$

The second term on the left side of the velocity boundary condition (14) accounts for the variation in the velocity of the interface due to the change in surface height. This term results in a coupling between the mean flow and the fluctuations, and this destabilizes the flow when the dimensionless parameter Γ increases beyond a critical value. The physical mechanism for the instability is the transfer of energy from the mean flow to the fluctuations due to the shear work done by the mean flow at the interface. When this rate of energy transfer exceeds the rate of viscous dissipation of energy in the fluid and the gel, the flow becomes unstable.
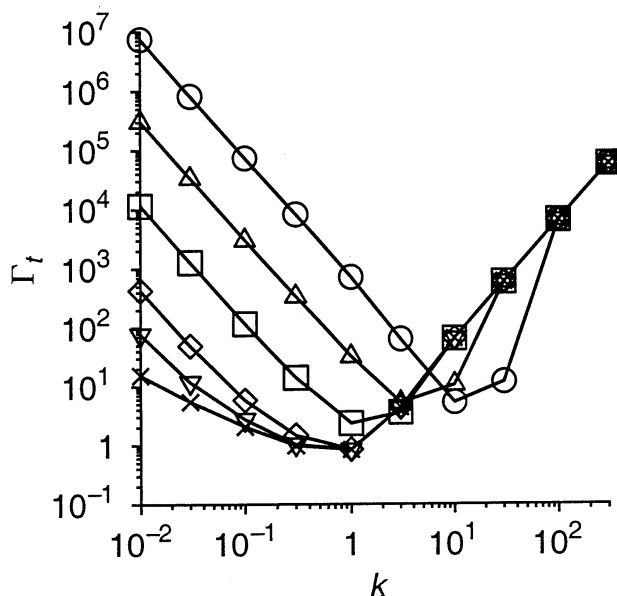
Figure 3. The dimensionless parameter Γ_t for transition from stable to unstable modes as a function of the wave number k for different values of the ratio of radii H and for $\mathbf{m} = 0$ for the flow in a flexible tube. ○, $H = 1.1$; △, $H = 1.3$; □, $H = 2$; ◇, $H = 5$; ▽, $H = 10$; ×, $H = 100$.

The typical neutral stability curves in the $\Gamma - k$ plane for the flow in a flexible tube (Figure 1 *b*) are shown in Figure 3 (ref. 16). The results are qualitatively similar for the plane Couette flow (Figure 1 *a*). It is observed that the neutral stability curve has a minimum at a finite value of wave number, and perturbations with this wave number become unstable when Γ is increased beyond a critical value. The results of the analysis for a plane Couette flow have been compared with experimental results[29,30], and agreement has been found with no adjustable parameters. An example of the comparison is shown in Figure 4 (for experimental details, see refs 29 or 30).

Inviscid instability

The inviscid instability occurs in the limit of high Reynolds number $Re \gg 1$ where the inertial stresses in the fluid are balanced by the elastic stresses in the wall material ($\mathbf{r}V^2/G) \sim 1$, or $Re \propto \Sigma^{1/2}$ where $\Sigma = (\mathbf{r}GR^2/\mathbf{m}^2)$. In this limit, the flow in a tube exhibits interesting behaviour[19,25,26]. The classical theorems of hydrodynamic stability of Rayleigh, Fjortoft and others were extended for this case by Kumaran[19] and Shankar and Kumaran[26].

These studies indicate that for a mean flow with mean velocity $\overline{v}_x = 0$ at the wall, the possibility of an instability depends on the parameter

$$H(r) = \overline{v}_x \frac{d}{dr}\left(\frac{r}{n^2 + k^2 r^2} \frac{d\overline{v}_x}{dr}\right). \tag{15}$$
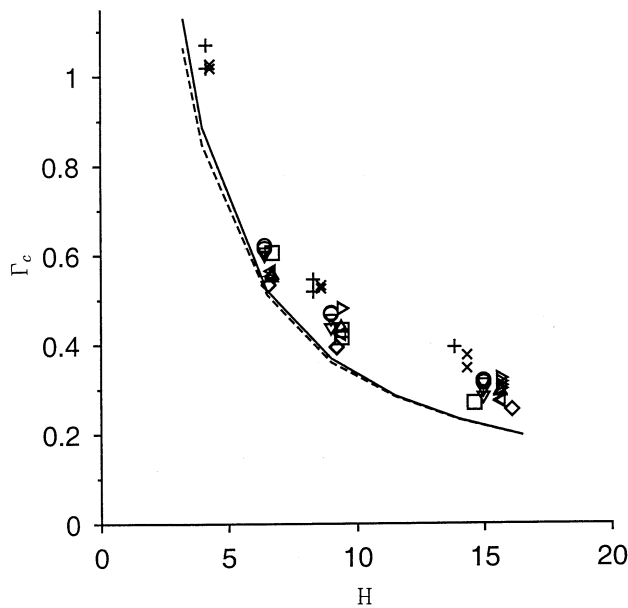
Figure 4. The dimensionless parameter Γ_c which is the minimum of the Γ_t vs k curve for the transition from stable to unstable modes as a function of the ratio of fluid and gel thicknesses H for different gels. Solid line – theoretical prediction for $G' = 4000$ Pa; broken line – theoretical prediction for $G' = 1000$ Pa; $\oplus$, $\circ$, $H = 4490$ μ, $G' = 2305$ Pa; $\square$, $H = 4699$ μ, $G' = 3788$ Pa; $\diamond$, $H = 4600$ μ, $G' = 4214$ Pa; $\triangle$, $H = 4690$ μ, $G' = 2642$ Pa; $\triangledown$, $H = 4490$ μ, $G' = 2354$ Pa; $\triangleleft$, $H = 4678$ μ, $G' = 4040$ Pa; $\triangleright$, $H = 4690$ μ, $G' = 3595$ Pa; $+$, $H = 4150$ μ, $G' = 947$ Pa; $\times$, $H = 4300$ μ, $G' = 1027$ Pa.

It can be shown that the flow could become unstable only if the parameter $H(r) < 0$ somewhere in the flow.

For a parabolic velocity profile and for axisymmetric perturbations $n = 0$, the parameter $H(r)$ is identically zero, and so there is no possibility of an instability. The asymptotic analysis of Kumaran[17] showed that in the leading order approximation, where viscous effects are neglected, the parabolic flow in a flexible tube is neutrally stable to axisymmetric perturbations. The correction to the growth rate due to viscous effects was calculated using an energy balance approach. It was found that there are two mechanisms of energy transfer – one due to the shear work done at the interface (which is the mechanism that destabilizes a viscous flow), and the transfer from the mean flow to the fluctuations due to the Reynolds stress term in the momentum equation. These two turn out to be equal in magnitude and opposite in direction, and therefore there is no net energy transfer from the mean flow to the fluctuations. However, there is a dissipation of energy due to the presence of a viscous wall layer of thickness $Re^{-1/2}$ at the wall, and this stabilizes the perturbations.

The factor $H(r)$ is negative for the developing flow in a tube of constant cross section, and the flow in a converging tube. The stability of these velocity profiles to axisymmetric perturbations was analysed by Shankar

and Kumaran[25]. In these flows, the inviscid stability equation (equivalent to the Rayleigh equation) has a singularity at a point where the wave speed is equal to the flow speed. In the 'critical layer' of thickness $Re^{-1/3}$ around this point, viscous stresses become important and it is necessary to incorporate viscous effects. These are included using asymptotic expansions[32], and the results indicate that the flow does become unstable when the Reynolds number exceeds a certain value. The mechanism of instability is the transfer of energy from the mean flow to the fluctuations due to the Reynolds stress terms in the critical layer. The instability Reynolds number has a minimum at a finite value of wave number k, and increases proportional to k^{-1} for $k \ll 1$ and proportional to k for $k \gg 1$. This is shown in Figure 5 (ref. 25), where the Reynolds number for transition from stable to unstable modes is shown as a function of the wave number k for a developing flow velocity profile when X, the ratio of the distance from the entrance and the radius of the tube, is 0.05. The critical Reynolds number, which is the minimum value of the Reynolds number for transition from stable to unstable modes, is found to increase proportional to $\Sigma^{1/2}$ in the limit of high Reynolds number, and shown in Figure 6 (ref. 25) for different distances from the entrance of the tube. Therefore, these modes are qualitatively different from the inviscid modes in a rigid tube, where the critical Reynolds number tends to a constant value in the limit of high elasticity.

The function $H(r)$ is also negative for parabolic flows in a flexible tube when the perturbations are non-axisymmetric ($n > 0$). The behaviour of the Reynolds number for the transition from stable to unstable modes
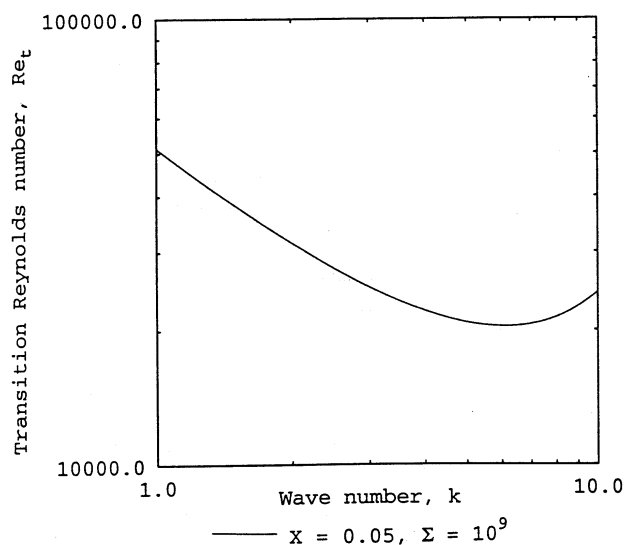

Figure 5. The Reynolds number for transition from stable to unstable modes as a function of wave number k for a developing flow velocity profile at a distance $X = 0.05$ from the entrance of the tube for $\Sigma = 10^9$ and $H = 2$.
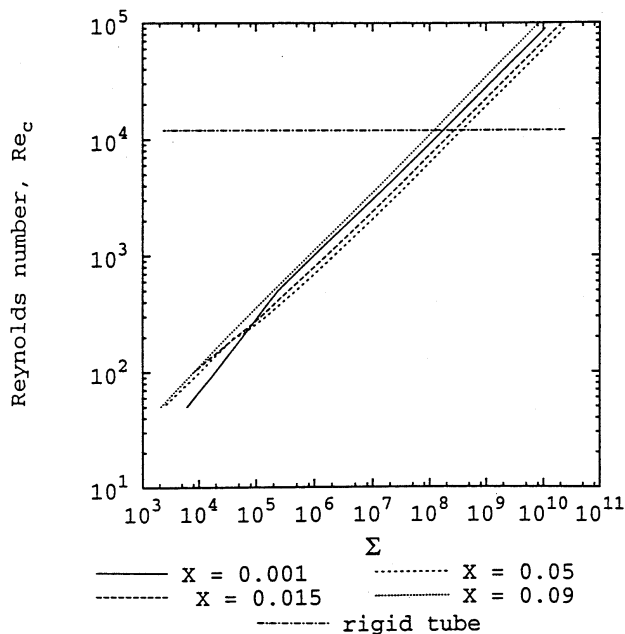
Figure 6. Critical Reynolds number as a function of $\Sigma = (\rho G R^2/\eta^2)$ for different values of X.
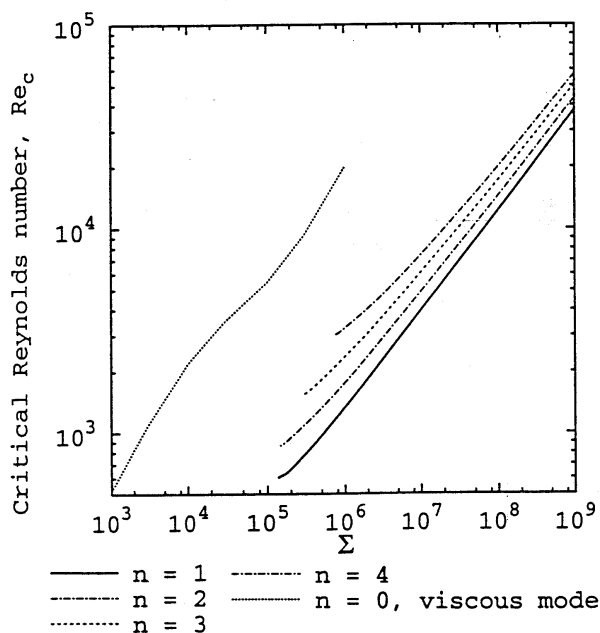

Figure 7. Critical Reynolds number for non-axisymmetric modes as a function of the parameter $\Sigma = (\rho G R^2/\eta^2)$ for a flexible tube with $H = 2$ and ratio of viscosities $\eta_r = 0$. The dotted line shows the continuation of the viscous mode from the low Reynolds number analysis.

as a function of the wave number k is similar to that for non-parabolic flows, and shows a minimum at a finite value of the wave number k. The critical Reynolds number, shown in Figure 7 (ref. 26), is a minimum for non-axisymmetric perturbations with azimuthal wave number $n = 2$. The dotted line shows the continuation of

the viscous modes from the low Reynolds number analysis, and it is seen that the inviscid mode has a lower critical Reynolds number than the continuation of the viscous mode.

5. Wall mode instability

The wall mode instability is observed in the limit of high Reynolds number, where the viscous stresses become important in a wall layer of thickness $O(Re^{-1/3})$ smaller than the macroscopic scale. The stability of the wall modes in the asymptotic regime $Re \propto \Sigma^{2/3}$ was analysed by Kumaran[22,24], and it was found that the wall modes are always stable in this regime. However, the asymptotic analysis of Shankar and Kumaran[27] showed that there is an instability in the asymptotic regime $Re \propto \Sigma^{3/4}$.

In contrast to the inviscid instability, the streamwise velocity in the wall layer for the wall modes is $O(Re^{-1/3})$ larger than that in the outer (inviscid) flow. Therefore, the velocity in the wall layer drives the outer flow, in contrast to the inviscid modes where the velocity in the outer flow is dominant. However, the force balances are rather subtle. The inertial and elastic stresses are of the same order of magnitude in the wall medium. The pressure forces due to the outer flow provide the dominant contribution to the normal force at the surface, even though the velocity in the outer flow is small compared to that in the wall layer. The ratio of the inertial forces
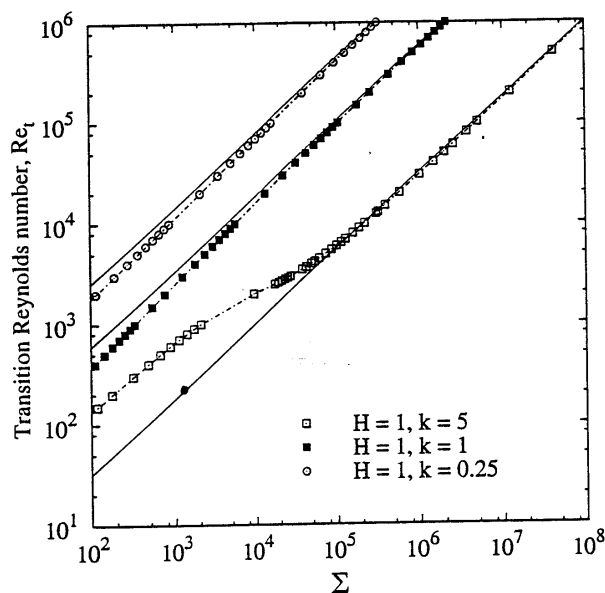

Figure 8. Comparison of the Reynolds number for transition from stable to unstable modes obtained from asymptotic results[27] (lines) with the intermediate Reynolds number numerical results[20] (dotted lines and symbols) of the Couette flow past a flexible surface. $\eta_r = 0$ for all cases plotted.
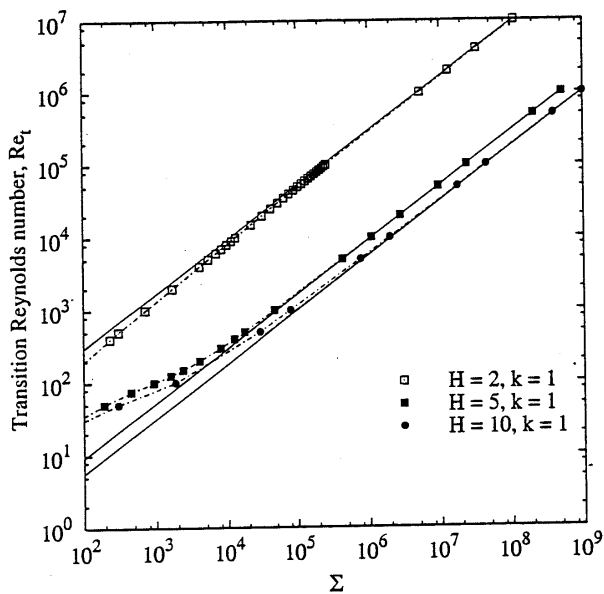
Figure 9. Comparison of the Reynolds number for transition from stable to unstable modes obtained from asymptotic results[28] (lines) with the intermediate Reynolds number numerical results[21] (dotted lines and symbols) of through a flexible tube. $m = 0$ for all cases plotted.
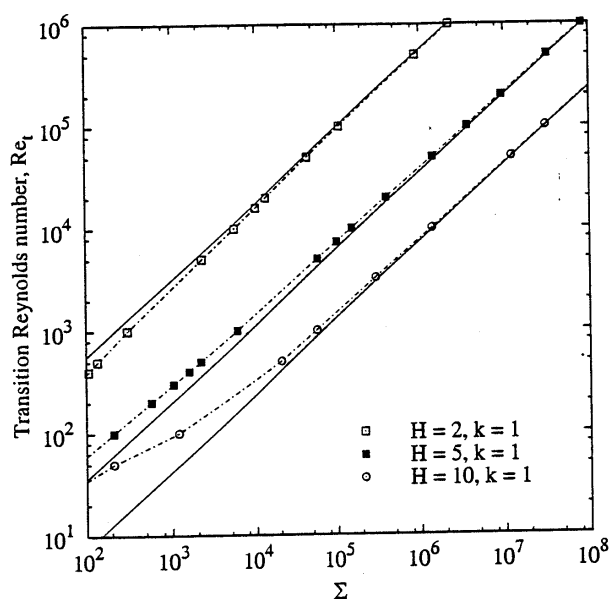

Figure 10. Comparison of the Reynolds number for transition from stable to unstable modes obtained from asymptotic results[28] (lines) with the numerical results obtained from the wall mode analysis[22] (dotted lines and symbols) of through a flexible tube. $m = 0$ for all cases plotted.

in the outer layer and the elastic forces in the wall medium is given by the dimensionless number $\Lambda = (rV^2/G)^{1/2}$. However, the flow does not become unstable when this number is $O(1)$ (refs 22, 24), but when this dimensionless number is of $O(Re^{1/3})$ (ref. 27), because the pressure force due to the outer flow is $O(Re^{1/3})$ larger than the tangential and normal stresses

in the wall layer. This implies a scaling $Re \propto \Sigma^{3/4}$ in terms of the dimensionless parameter $\Sigma = (rGR^2/R^2)$ for these modes. This is higher than the scaling $Re \propto \Sigma^{1/2}$ for the inviscid modes, and consequently these modes are more stable than the inviscid modes. However, this instability is likely to be observed in specific cases, such as the Couette flow in a channel (Figure 1 *a*) where there is no inviscid instability.

A comparison between the asymptotic analysis of Shankar and Kumaran[27,31] and previous numerical results[20–22] is shown in Figures 8–10. It is seen that the asymptotic analysis accurately captures the neutral stability curves for the Couette flow in a channel[20] at intermediate Reynolds numbers, as well as the wall modes[22] for the flow in a tube at intermediate Reynolds numbers and the continuation of the viscous modes in a tube at intermediate Reynolds number[21].

6. Conclusions

The instabilities of the flow in flexible tubes and channels have been classified on the basis of the asymptotic regime where they are observed, the destabilizing mechanism and the flow structure of the neutrally stable perturbations. These are

1. The *viscous modes*, which are observed in the limit of low Reynolds number $Re \ll 1$. The critical Reynolds number for these modes follows the scaling law $Re \propto \Sigma$, where the dimensionless parameter $\Sigma = (rGR^2/m)$ is independent of the fluid velocity. Though this scaling law is anticipated from dimensional analysis, it is necessary to carry out the stability calculations to determine whether the flow can become unstable. There is a balance between the viscous forces in the fluid and the elastic forces in the wall material in this regime, and inertia in the fluid and the wall material is negligible. The destabilizing mechanism in this case is the transfer of energy from the mean flow to the fluctuations due to the shear work done by the mean flow at the interface.

2. The *inviscid modes* in the limit $Re \gg 1$ and $Re \propto \Sigma^{1/2}$, where there is a balance between the inertial forces in the fluid and the elastic forces in the wall material. Though the scaling is predicted by dimensional analysis, the linear stability analysis indicated that the flow becomes unstable only in certain situations such as for axisymmetric perturbations in developing flows and flows in converging tubes, and for non-axisymmetric perturbations in a fully developed flow. These modes are characterized by the presence of a critical layer of thickness $Re^{-1/3}$ in the flow where the viscous stresses become important. The destabilizing mechanism is the transfer of energy due to the Reynolds stresses in the

critical layer. However, these modes are not a continuation of the Tollmien–Schlichting instability in rigid tubes and channels, since the critical Reynolds number is proportional to $(\rho G R^2/\eta^2)^{1/2}$ in the limit of large elasticity, whereas the critical Reynolds number of the Tollmien-Schlichting modes converges to a finite value in this limit.

3. The *wall mode* instability which is observed in the limit $Re \gg 1$ and $Re \propto \Sigma^{3/4}$. In this case, there is a viscous wall layer of thickness $Re^{-1/3}$ at the flexible surface, and the destabilizing mechanism is the transfer of energy from the mean flow to the fluctuations due to the shear work done by the mean flow at the interface. The presence of tangential motion in the wall material is essential for inducing this instability.

1. Kramer, M. O., *J. Aero. Sci.*, 1957, **24**, 459.
2. Kramer, M. O., *J. Am. Soc. Naval Engrs.*, 1960, **74**, 25.
3. Carpenter, P. W. and Garrad, A. D., *J. Fluid Mech.*, 1985, **155**, 465.
4. Carpenter, P. W. and Garrad, A. D., *J. Fluid Mech.*, 1986, **170**, 199.
5. Benjamin, T. B., *J. Fluid Mech.*, 1960, **9**, 513.
6. Benjamin, T. B., *J. Fluid Mech.*, 1963, **16**, 436.
7. Landahl, M. T., *J. Fluid Mech.*, 1962, **13**, 609.
8. Tollmien, W., *1. Mitt., Ges. Wiss. Gottingen, Math. Phys. Klasse 21*, 1929.
9. Schlichting, H., *Z. Agnew. Math. Mech.*, 1933, **13**, 171.
10. Carpenter, P. W. and Gajjar, J. S. G., *Theor. Comput. Fluid Dynamics*, 1990, **1**, 349.
11. Carpenter, P. W., *Prog. Astro. Aero.*, 1990, **123**, 79.
12. Green, C. H. and Ellen, C. H., *J. Fluid Mech.*, 1972, **51**, 403.
13. Lin, C. C., *Q. Appl. Math.*, 1945, **3**, 117–142, 218–234, 277–301.
14. Krindel, P. and Silberberg, A., *J. Colloid Interface Sci.*, 1979, **71**, 34.
15. Kumaran, V., Fredrickson, G. H. and Pincus, P., *J. Phys. France II*, 1994, **4**, 893–911.
16. Kumaran, V., *J. Fluid Mech.*, 1995, **294**, 259–281.
17. Kumaran, V., *J. Chem. Phys.*, 1995, **102**, 3452–3460.
18. Kumaran, V., *J. Fluid Mech.*, 1995, **302**, 117–139.
19. Kumaran, V., *J. Fluid Mech.*, 1996, **320**, 1–17.
20. Srivatsan, L. and Kumaran, L., *J. Phys. II (France)*, 1997, **7**, 947–963.
21. Kumaran, V., *J. Fluid Mech.*, 1998, **357**, 123–140.
22. Kumaran, V., *J. Fluid Mech.*, 1998, **362**, 1–15.
23. Kumaran, V. and Srivatsan, L., *Euro. Phys. J. B.*, 1998, **2**, 259–266.
24. Kumaran, V., *Euro. Phys. J. B.*, 1998, **4**, 519–527.
25. Shankar, V. and Kumaran, V., *J. Fluid Mech.*, 1999, **395**, 211–236.
26. Shankar, V. and Kumaran, V., *J. Fluid Mech.*, in press.
27. Shankar, V. and Kumaran, V., *J. Fluid Mech.*, submitted.
28. Shankar, V. and Kumaran, V., *Euro. Phys. J. B.*, submitted.
29. Kumaran, V. and Muralikrishnan, R., *Phys. Rev. Lett.*,
30. Muralikrishnan, R. and Kumaran, V., *Phys. Fluids*, submitted.
31. Shankar, V. and Kumaran, V., *J. Fluid Mech.*, submitted.
32. Drazin, P. G. and Reid, W. H., *Hydrodynamic Stability*, Cambridge University Press, Cambridge, 1981.